First Identification of an Aliphatic cis-α,β-Dinitroso Compound: A Combined Experimental and Quantum Chemical Study

Hans-Jörg Himmel,*,† Serge Konrad,‡ Willy Friedrichsen,‡ and Guntram Rauhut*,§

Institut für Anorganische Chemie, Universität Karlsruhe, Engesserstrasse, Geb. 30.45, 76128 Karlsruhe, Germany, Institut für Organische Chemie, Universität Kiel, Otto-Hahn-Platz 4, 24098 Kiel, Germany, and Institut für Theoretische Chemie, Universität Stuttgart, Pfaffenwaldring 55, 70569 Stuttgart, Germany

Received: January 16, 2003; In Final Form: June 25, 2003

A combination of experimental and quantum chemical results has been used to characterize dimethylfuroxan, $(CH_3)_2C_2N_2O_2$, isolated in a matrix of solid Ar atoms at 12 K, and then to study its photoinduced isomerization and decomposition. The less-stable isomer 2,3-dinitrosobut-2-ene can be generated by UV photolysis ($\lambda_{max} = 254$ nm). However, this species is photolabile and decomposes upon prolonged photolysis times with light having $\lambda_{max} = 254$ nm or with IR radiation ($\lambda_{max} = 700$ nm) to give CH_3CNO as the final, photostable product. The two photoproducts were characterized using a combination of experimental and quantum chemical results. The work presented herein sheds light on the physical and chemical properties of furoxans, which may gain considerable importance as a source of NO, which itself plays a significant role as a biological messenger.

Introduction

Furoxans (1,2,5-oxadiazole-2-oxides) are of considerable interest as possible sources of nitric oxide, which plays an important role as a biological messenger.[1,2] In the past, the ring-opening process of furoxans leading to the dinitroso isomer, which was found to be less stable in many cases, has been studied in some detail.[3−11] For example, it has been shown that $C_6H_4N_2O_2$ is stable as benzofuroxan under normal conditions, but the matrix-isolated molecule can be transformed at very low temperatures (10−20 K) into dinitrosobenzene by the action of selective photolysis at $\lambda_{max} = 366$ nm.[12−14] The gain of resonance energy of the benzene ring does not compensate for the energy needed to open the furoxan ring, and therefore, dinitrosobenzene is less stable than benzofuroxan. Dinitrosobenzene itself can adopt several configurations depending on the dihedral angles of the nitroso groups. The analysis of these configurations is important because it allows for conclusions regarding the mechanism of the ring-opening process.

Herein, we discuss a possible photolytically activated ring-opening reaction of dimethylfuroxan to give 2,3-dinitrosobut-2-ene. Because of the lack of aromatic stabilization in 2,3-dinitrosobut-2-ene, this species is expected to be a high-energy species, and the energy required for ring opening should exceed significantly the one required in the case of benzofuroxan.[15,16] Again, the product of the ring-opening reaction can adopt several isomeric forms, and the experimental results should allow us to discriminate between these isomers. A first gas-phase study gives some hints about possible products. Recently, Pasinszki and Westwood studied the thermal decomposition of dimethylfuroxan at 600 °C in the gas-phase, and the authors identified acetonitrile-*N*-oxide as the only traceable product of this decomposition in their IR and HeI photoelectron spectra.[17] This product was previously sighted in matrix experiments as one of the products of the reaction between CH_3CN and O_2.[18] Especially noteworthy is that Pasinszki and Westwood found no experimental evidence for possible intermediates such as the ring-opening product 2,3-dinitrosobut-2-ene. In addition, the authors analyzed theoretically possible mechanisms, in these relying on the B3LYP density functional in combination with a 6-31G* type basis set. On the basis of these theoretical studies, the authors discussed the possibility of a mechanism that includes (i) a ring opening of the dimethylfuroxan, (ii) rotation around the C1−C2 bond, and finally (iii) cleavage of the C1−C2 bond and formation of two acetonitrile-*N*-oxide moieties. The barrier height for the ring opening process was found to be the rate-determining step in the decomposition of dimethylfuroxan and was calculated to be 215.9 kJ mol^{-1}.

According to these calculations, there is little hope that 2,3-dinitrosobut-2-ene can be stabilized under "normal" conditions. However, the matrix technique has proved before its capability to retain intermediates of this kind. The low temperatures of about 10 K (for which $kT = 0.08$ kJ mol^{-1} and a barrier of only 5 kJ mol^{-1} cannot be overcome by thermal means, if tunneling processes can be neglected) and the fixation in the matrix cage are factors that are in favor for the experimental detection of such an intermediate. Herein it will be shown that our experiments indeed succeed to give for the first time experimental evidence for the formation of 2,3-dinitrosobut-2-ene as a reactive intermediate during the photolytically induced decomposition of dimethylfuroxan. Moreover, it will be shown how a combination of experimental and theoretical results lead to a detailed analysis of the structure of the configuration of the 2,3-dinitrosobut-2-ene formed. The implications for the mechanism will be discussed.

Experimental Details

3,4-Dimethylfuroxan was synthesized as reported previously.[19] The product was characterized by its NMR spectrum [^{1}H NMR (200 MHz, $CDCl_3$): $\delta = 2.33$ (s), 2.15 (s) ppm].

* To whom correspondence should be addressed.
† Universität Karlsruhe.
‡ Universität Kiel.
§ Universität Stuttgart.

10.1021/jp0341117 CCC: $25.00
Published on Web 07/31/2003

Matrix Experiments. In a high-vacuum apparatus, the compound (kept at 0 °C) was slowly and over a period of 2 h sprayed through a glass nozzle together with an excess of Ar gas onto a freshly polished Cu block kept at 12 K by means of a closed-cycle refrigerator (Leybold LB510), resulting in an Ar matrix containing ca. 5% of dimethylfuroxan. Additional experiments were carried out in which the temperature of the compound was varied in the temperature range −20 to 25 °C, resulting in matrixes containing different proportions of dimethylfuroxan. These experiments showed that no significant absorptions due to two interacting dimethylfuroxan moieties can be traced for concentrations up to 5% of furoxan. For this concentration, the intensities of the bands were optimal after 2 h of deposition, and thus, we report in the following the experiments for this concentration. The experiments with lower concentrations follow the same pattern. After characterization by its IR spectrum, the matrix was subjected to several cycles of UV photolysis (at $\lambda_{max} = 254$ nm). To monitor the effects of photolysis, an IR spectrum of the matrix was recorded after each of these photolysis cycles. Details about the relevant procedures and experimental techniques used in our experiments are given elsewhere.[20−22]

IR spectra were taken with the aid of a Bruker 113v spectrometer equipped with a liquid N_2 cooled MCT and a DTGS detector for measurements in the range 4000−200 cm^{-1} with a resolution of 1 cm^{-1}. Photolysis was achieved with a low-pressure Hg lamp (Graenzel, Karlsruhe) operating at 200 W, the radiation being transmitted through a quartz window.

Computational Details. The geometries of all structures were optimized at the B3LYP/cc-pVTZ and the B3LYP/6-31G* levels using the Gaussian 98 code.[23−25] After the harmonic force field was calculated, the Cartesian force constants were transformed into a basis of natural internal coordinates following the suggestions of Pulay et al.[26] To account for anharmonicities, basis set deficiencies and lacking contributions to the electron correlation the force constants were scaled by a set of 10 factors being optimized for sets of structurally related internal coordinates. Eight of these factors were taken from the set of transferable scaling factors reported in ref 27. The other two, namely, those corresponding to all C−C and C−N bonds, were reoptimized by a least-squares procedure on the basis of all experimentally securely assigned frequencies within this study to account for the unusual structural motifs of the molecule studied here. These scaling factors were optimized to 0.98 and 0.89, respectively. This procedure has been successfully applied previously for the analysis of the vibrational spectra of furoxan and its halogenated derivatives.[28,29] For these species, the absolute mean deviation between the calculated and the experimental spectra was found to be less than 10 cm^{-1} in all cases. Because the scaling of the force constant matrix affects not only the eigenvalues of the Hessian but also the eigenvectors, the IR intensities are usually improved by this procedure as well.

Results of the Matrix Isolation Experiments

Figure 1a shows a typical IR spectrum of an Ar matrix containing dimethylfuroxan. The strongest absorption in the spectrum occurs at 1623 cm^{-1}. This value is close to one of the strongest absorptions in the IR spectrum of matrix-isolated benzofuroxan (1622 cm^{-1}),[30] for which the corresponding mode was approximately described as a combination of both the ν(C−N) and the ν(N−O) stretching fundamentals. Therefore, the detection of this absorption indicates the presence of an intact furoxan ring.

Figure 1b displays the IR spectrum after exposure of the matrix to a period of 2 h of UV photolysis ($\lambda_{max} = 254$ nm).

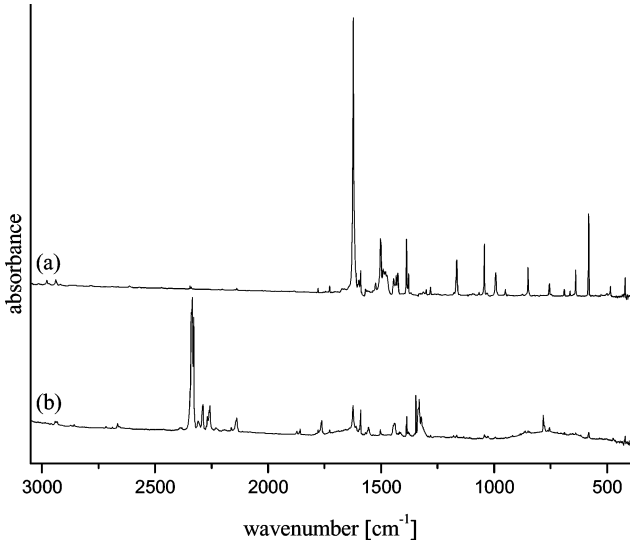

Figure 1. IR spectra of an Ar matrix containing dimethylfuroxan: (a) before photolysis; (b) following 2 h of UV photolysis ($\lambda_{max} = 254$ nm).

The absorptions due to dimethylfuroxan were observed to decrease sharply. At the same time, several new absorptions grew in. The strongest of these new absorptions was located at 2338 cm^{-1}. Additional smaller absorptions appeared at 1344, 1321, and 783 cm^{-1}. Thus, the experiments indicate that photolysis leads to decomposition of dimethylfuroxan and formation of at least one photoproduct, **A**.

In additional experiments, the photolysis time was modified and IR spectra were recorded for several exposure times of the matrix to the photolysis. Figure 2 displays the IR spectra in the two regions 840−770 and 1270−1200 cm^{-1} upon deposition and following 10, 30, 60, 90, 150, 215, 275, 395, 695, 995, 1295, 1895, and 3600 s of UV−photolysis ($\lambda_{max} = 254$ nm). As visible in Figure 2a, a large and intense absorption grew in at 783 cm^{-1}, which belongs to the photoproduct **A**. The absorption was clearly visible after 215 s of photolysis and then continuously increased in intensity for longer photolysis times until, at 3600 s, it reached its maximum. Exposure times longer than 3600 s led to no significant further changes. A smaller absorption was seen to grow in at 825 cm^{-1}. However, it showed a distinctively different behavior toward photolysis. It already started growing for very short photolysis times and reached its maximum intensity at about 395 s of photolysis. After this, it decreased again in intensity until it completely vanished again for photolysis times longer than 3600 s. Thus, the species responsible for this absorption belongs in all certainty to a second distinct photoproduct **B** of the photolytically induced decomposition of dimethylfuroxan. Figure 2b shows another absorption, located at 1239 cm^{-1}, that showed the same behavior as the band at 825 cm^{-1}, and therefore, most likely belongs to the same species **B**, which is generated and again consumed in the course of photolysis.

Finally, experiments were conducted in which the energy of photolysis was modified. Dimethylfuroxan showed no photochemistry in the visible region (400−800 nm). Thus the electronic transition that initiates decomposition most likely lies in the UV region. Modification of the photolysis energy influences the reaction kinetics. However, it was not possible to find photolysis conditions under which species B was generated and photostable without the appearance of the absorptions characteristic of photoproduct **A**. The obvious inference of all experiments is that **B** is an intermediate product on the way to the photostable end product **A**.

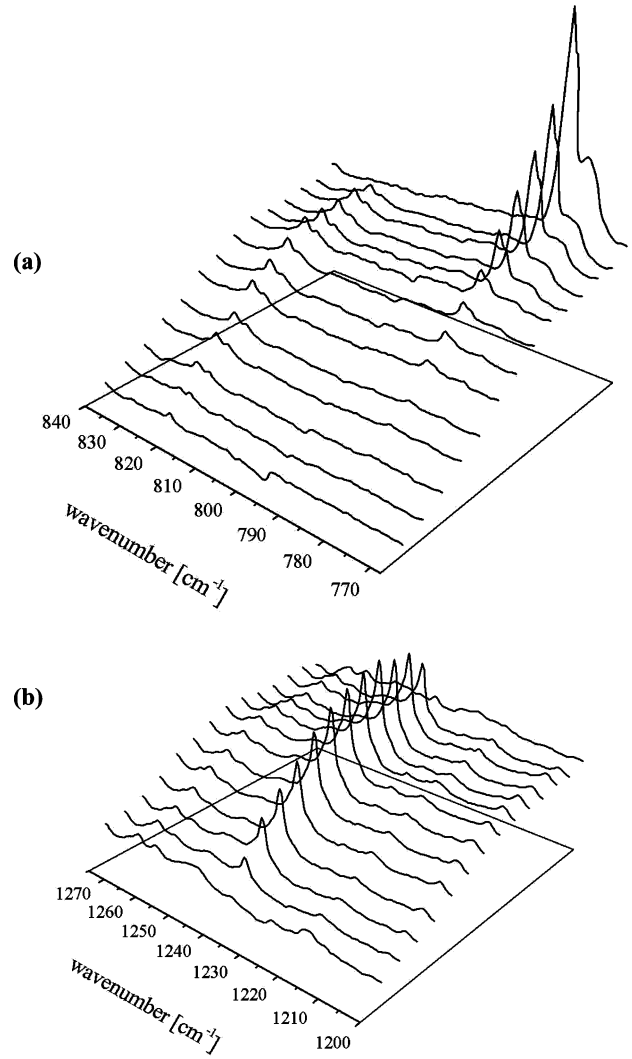

Figure 2. IR spectra in the regions around (a) 800 and (b) 1230 cm^{-1} taken after deposition of dimethylfuroxan in an Ar matrix and different UV photolysis times of the matrix (see text). Offsets were added to the baselines in these plots to show the time effects more clearly.

TABLE 1: Selected Structural Parameters of 3,4-Dimethylfuroxan (B3LYP/cc-pVTZ)

parameter	bond length [Å]	parameter	angle [deg]
r(C1−C2)	1.422	∠(C3−C1−C2)	127.4
r(C1−C3)	1.496	∠(C4−C2−C1)	132.0
r(C2−C4)	1.491	∠(C1−C2−N2)	106.6
r(C1−N1)	1.310	∠(C2−C1−N1)	111.4
r(C2−N2)	1.331	∠(C1−N1−O1)	107.2
r(N1−O1)	1.371	∠(C2−N2−O1)	106.8
r(N2−O1)	1.452	∠(C2−N2−O2)	134.7
r(N2−O2)	1.225	∠(N1−O1−N2)	107.9

Discussion

In the following, a combination of experimental and quantum chemical results will be used to identify and characterize dimethylfuroxan and its photoproducts **A** and **B**. It will be shown that **B** can be identified as *trans-cis-trans*-2,3-dinitrosobut-2-ene and **A** as (the previously already sighted species) CH_3CNO.

Dimethylfuroxan. Calculations were first employed to calculate the structure and IR properties of dimethylfuroxan. Table 1 contains the most important geometrical parameters of the molecule in its global energy minimum structure, exhibiting C_s symmetry. A typical feature of all furoxans is the unusually long endocyclic N2−O1 bond, which amounts to 1.452 Å. At 1.422 Å, the C1−C2 distance is shorter than the distance expected for a single bond.

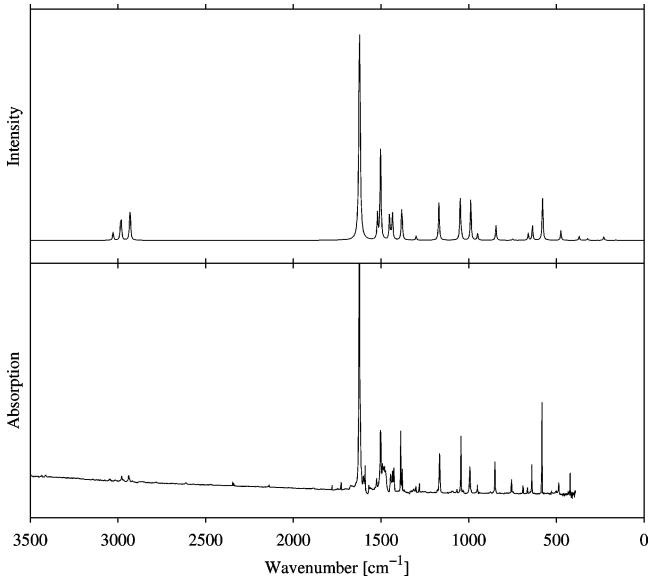

Figure 3. Simulated SQM/B3LYP IR spectrum of dimethylfuroxan (top), together with the experimentally obtained one (bottom).

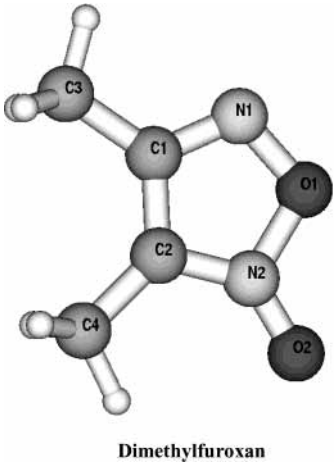

The calculated vibrational spectrum is displayed in Figure 3, together with the experimental one. From the comparison between observed and calculated spectra, it is clear that the agreement between them is pleasing. The calculations succeed in predicting not only the correct wavenumbers for all of the modes but also the correct relative intensities for most of the vibrational modes. Table 2 contains a comparison of all observed and calculated wavenumbers. The strongest absorption in both the experimental and calculated spectra, which belongs to a mode that can approximately be described as a combination of both the ν(C−N) and the ν(N−O) stretching fundamentals, is observed at 1623 cm^{-1} and calculated to show at 1622.2 cm^{-1}. The strong absorption at 581 cm^{-1} in the experimental and at 578.5 cm^{-1} in the calculated IR spectrum belongs to a mode that can roughly be described as a ring-bending mode. The strong feature observed at 1166 cm^{-1} and calculated at 1169.5 cm^{-1} can be assigned to a mode with high character of the CCH bending mode and the ν(C−C) stretching mode.

CH_3CNO, A. As shown recently by Pasinszki and Westwood, thermolysis of dimethylfuroxan leads to acetonitrile-*N*-oxide. Guided by the work of these authors, we have calculated the energy minimum structure and vibrational properties of this species. Table 3 compares the observed wavenumbers of **A** with

TABLE 2: Comparison between the IR Properties of Dimethylfuroxan Observed and Calculated[a]

obsd	intensity[b]	calcd	intensity	approximate description
3049	w	3028.4	4	CH str
3041	w	3025.4	2	CH str
2978	w	2985.3	10	CH str
2968	vw	2980.5	12	CH str
2938	w	2932.6	14	CH str
2918	vw	2928.9	13	CH str
1623	vs	1622.2	332	exocycl NO str and CN str
1526	w	1519.9	18	CNstr
1502	m	1502.4	76	CC str (ring)
1484	broad, m	1453.1	0.1	HCH bend
1445		1451.5	17	HCH bend
1433		1442.9	3	HCH bend
1426		1434.3	18	HCH bend
1387		1382.3	18	HCH bend
1379		1378.5	8	HCH bend
1281	m	1299.4	3	ring def
1166	s	1169.5	27	CCH-bend and CCstr
1066	w	1057.7	0.3	CCH-bend
1045	s	1047.9	29	CCH-bend and ring def
1032	w	1039.5	2	CCH-bend
992	s	988.0	29	CCH-bend and ring def
950	m	949.0	5	CCH-bend and ring def
850	s	844.2	10	endocycl NO str and ring def
755	m	748.9	1	C−C(Me) str and ring def
664	m	660.2	4	ring torsion and NO oop
640	s	635.9	10	ring def
585	shoulder	582.5	0.2	ring torsion and NO oop
581	vs	578.5	31	ring bend
485	m	474.2	6	endocycl NO str
		369.7	3	ring torsion
318	w	321.9	1	Me bend
300	w	265.4	0.04	Me oop mode
		229.4	2	Me bend
		160.3	0.2	ring torsion
		124.8	0.01	Me torsion
		36.9	0	Me torsion

[a] Wavenumbers in cm^{-1}; calculated IR intensities in km mol^{-1}. [b] w = weak; m = middle; s = strong; vs = very strong in intensity.

TABLE 3: Comparison between the IR Properties Observed and Calculated for CH_3CNO[a]

expt	intensity	calcd	intensity	gas phase[17]	matrix[18]	assignment
		2975.6	4	3022.5		CH str
		2975.1	4	2950 R 2935 P		CH str
		2904.6	22			CH str
2338	s	2338.5	386	2311	2309	CN str
		1385.8	9	1453.2		HCH bend
		1385.5	9	1401 R 1386 P	1381	HCH bend
1344	s	1376.1	120			NO str and CC str
1321	s	1324.3	67	1356 R 1348.9 Q 1346.3 Q 1340 P	1332	HCH bend
		1005.5	2			CCH bend
		1004.4	2			CCH bend
783	m	782.9	22	791 R 788.1 Q 781.9 Q 777 P	780	CC str
		478.7	7	477.3		linear deform
		478.7	7			linear deform
		115.6	2	150 ± 50		linear deform
		115.2	2			linear deform

[a] Wavenumbers in cm^{-1}; intensities in km mol^{-1}.

the calculated ones for CH_3CNO. The vibrational spectrum of acetonitrile-*N*-oxide has been discussed in detail by Pasinszki and Westwood. A comparison between the published data of these authors and our results strongly suggests that **A** can be identified as CH_3CNO. This species was previously sighted in matrix experiments.[18] The wavenumbers measured herein slightly deviate from these earlier values but are in better agreement with the gas-phase data. Because diffusion from the matrix side generally is very limited, the most likely explanation for the deviation is that the molecule interacts in the previously reported experiments to some extent with another species being trapped in the same cage of the polycrystalline Ar matrix. The data might suggest that interaction is stronger for the previously studied CH_3CNO species (which was generated from CH_3CN and O_2)[18]

In the case of matrix experiments starting with benzofuroxan, the furoxan ring opening leading to the dinitroso isomer was the only detectable reaction upon photolysis. Dinitrosobenzene was found to be photostable. On the basis of our results, it is likely that 2,3-dinitrosobut-2-ene is not stable towards decomposition into two CH_3CNO moieties.

2,3-Dinitrosobut-2-ene, B. As already mentioned, it was previously shown that benzofuroxan can be transformed into its isomer dinitrosobenzene by UV photolysis. The analogue product of the possible photoinduced isomerization of dimethylfuroxan is 2,3-dinitrosobut-2-ene. This species can adopt several configurations in dependence of the dihedral angles involving the nitroso groups. Formally, one would expect six local minima corresponding to different conformers on the potential energy surface. To keep the terminology as simple as possible, these are labeled *ccc*-2,3-DNB, *cct*-2,3-DNB, *tct*-2,3-DNB, *ctc*-2,3-DNB, *ctt*-2,3-DNB, and *ttt*-2,3-DNB, where *c* denotes cis orientation and *t* the corresponding trans orientation of the nitroso and methyl groups (see Chart 1). In agreement with our studies on unsubstituted furoxan (see ref 16), *ccc*-2,3-DNB was found to be a transition state rather than a local minimum and *cct*-2,3-DNB is not a stationary point on the hypersurface. Consequently, 2,3-dinitrosobut-2-ene allows for four conformational isomers only. The conformer lowest in energy at the B3LYP/cc-pVTZ level is *ttt*-2,3-DNB (see Table 4). However, starting from the planar furoxan ring, this

CHART 1: The Possible Conformers of 2,3-Dinitrosobut-2-ene and Their Short Notation, Which Is Used in the Discussion

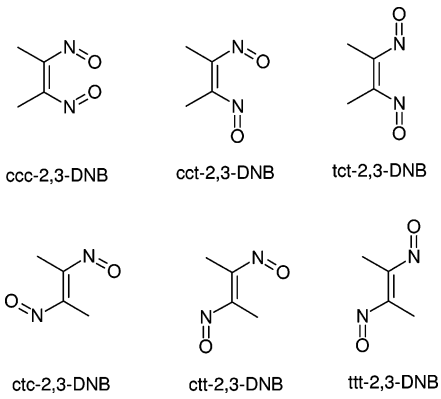

TABLE 4: Energies [kcal/mol] of the Conformers of 2,3-Dinitrosobut-2-ene Relative to Dimethylfuroxan

species	relative energy	ZPVE
dimethylfuroxan	0.0	65.7
tct-2,3-DNB	32.4	63.2
ctc-2,3-DNB	38.1	63.3
ctt-2,3-DNB	32.8	63.5
ttt-2,3-DNB	28.0	63.8

conformer would require a rotation about the central C1−C2 bond, which appears to be unlikely in the Ar cage. Therefore, the most likely structure to be observed in the matrix is the conformer with both nitroso groups on the same side of the double bond, that is, *tct*-2,3-DNB. According to our calculations,

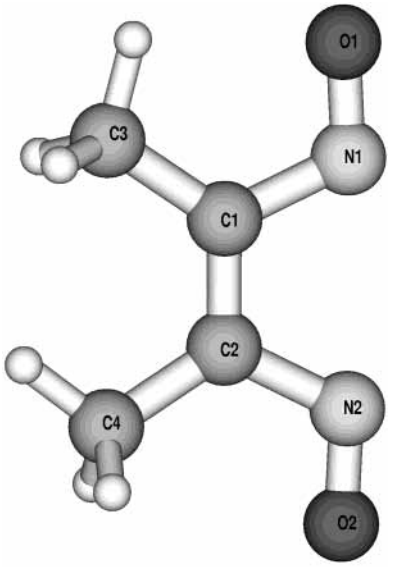

***tct*-2,3-DNB**

the most intense bands in the spectrum of *tct*-2,3-DNB should occur at 1530.8, 1515.6, 1224.1, and 814.1 cm^{-1}. Of these, the bands at 1224.1 and 814.1 cm^{-1} occur in a region that is free of any absorptions belonging to furoxan. As already mentioned, in our experiments, absorptions at 1239 and 825 cm^{-1} (belonging to the photoproduct **B**) are clearly seen to first grow in on photolysis and then vanish again if the photolysis time is increased. On these grounds, we can identify species **B** as *tct*-2,3-DNB. The calculated wavenumbers for all four conformers are summarized in Table 5. The calculated spectra are visualized in Figure 4. The most intense feature in the experimental spectrum of **B** is the band at 1239 cm^{-1} (see also Figure 2). All possible structures exhibit vibrational modes in this region. However, for two of these structures, the IR intensities of these modes are zero, because the net change of the dipole moment for these modes is zero due to the symmetry of the molecule (center of inversion). In the third structure, the intensity of the mode (at 1222.5 cm^{-1}) is not zero but is significantly smaller than several others absorptions that should be detectable subject to this species being formed in significant yields in our experiments. However, in the experiments, there is no sign of any other of these bands. On the other hand, the absorption at 1224.1 cm^{-1} in the spectrum of *tct*-2,3-DNB is predicted to carry the most intensity of all absorptions, in pleasing agreement to the experiments.

Thus, the sum of all experimental and calculational results indicates that *tct*-2,3-DNB is the photolabile intermediate during the decomposition of dimethylfuroxan leading finally to CH_3-CNO. This result is in agreement with our recent computational study on the thermally induced molecular rearrangement of furoxan.[16] Figure 5 shows the experimental spectrum obtained upon 5 min UV photolysis of an Ar matrix containing dimethylfuroxan, together with the superposition of the calculated IR spectra for dimethylfuroxan, *tct*-2,3-DNB, and CH_3-CNO. As can be seen from this figure, the calculations succeed in reproducing nicely the experimentally observed spectrum.

TABLE 5: Wavenumbers (in cm^{-1}) and IR Intensities (in km mol^{-1}) of the Conformers of 2,3-Dinitrosobut-2-ene Obtained from SQM/B3LYP Calculations

	tct-2,3-DNB		*ctc*-2,3-DNB		*ctt*-2,3-DNB		*ttt*-2,3-DNB	
no.	υ	int	υ	int	υ	int	υ	int
36	3044.2	6.5	3019.3	9.1	3066.3	0.5	3067.8	0.2
35	3035.4	4.6	3019.1	1.7	3033.1	3.5	3067.6	1.6
34	2989.0	0.5	2996.8	12.1	2998.5	5.6	2988.4	10.7
33	2987.4	9.0	2996.2	0.0	2980.8	6.8	2988.2	0.0
32	2940.5	2.0	2939.7	9.5	2941.9	3.3	2941.9	6.3
31	2935.4	4.5	2939.3	0.2	2928.2	6.1	2941.5	0.1
30	1668.1	18.2	1597.0	0.0	1632.2	4.0	1672.3	0.0
29	1530.8	130.8	1504.1	328.5	1518.3	201.4	1525.3	0.0
28	1515.6	100.3	1467.5	0.0	1502.6	68.9	1515.1	271.4
27	1461.4	6.0	1452.6	23.3	1452.3	19.5	1442.6	16.7
26	1444.2	22.4	1450.5	0.0	1447.0	4.1	1438.5	0.0
25	1431.2	10.3	1423.8	25.8	1434.9	3.1	1437.6	6.0
24	1426.5	3.5	1422.2	0.0	1416.9	8.9	1427.5	0.0
23	1371.8	32.4	1379.1	18.5	1373.1	19.1	1367.1	41.1
22	1361.7	35.8	1376.3	0.0	1366.5	4.7	1366.6	0.0
21	1224.1	231.3	1216.9	0.0	1222.5	32.5	1232.5	0.0
20	1120.0	4.9	1150.4	9.0	1133.6	49.9	1138.9	131.5
19	1094.4	7.8	1046.5	60.9	1067.4	51.1	1081.3	46.0
18	1036.8	0.0	1029.8	17.6	1045.9	2.7	1036.8	3.9
17	992.4	7.7	1020.5	0.0	1018.4	16.6	1017.4	0.0
16	941.8	42.2	933.2	0.0	932.1	13.9	950.8	0.0
15	814.1	98.8	881.9	79.0	838.3	96.4	838.2	175.7
14	774.6	22.8	713.3	0.0	771.4	8.7	772.0	0.0
13	703.3	2.1	640.1	0.0	677.9	1.1	719.9	1.6
12	551.2	0.0	608.5	1.4	582.1	2.1	542.5	0.0
11	474.3	0.5	490.4	0.0	506.6	2.3	511.0	0.0
10	430.4	7.7	401.8	6.5	408.7	1.0	418.2	0.0
9	358.9	1.3	378.0	0.0	378.3	3.3	357.6	2.6
8	355.6	1.4	286.6	1.7	319.3	2.3	342.1	4.7
7	333.0	2.0	272.8	0.0	299.3	0.6	316.4	0.0
6	207.5	1.8	255.3	10.4	232.9	12.2	221.6	11.0
5	207.3	0.0	207.1	0.0	185.7	2.7	187.4	0.0
4	106.1	0.0	200.0	9.5	171.1	2.4	177.0	0.7
3	77.0	0.0	120.6	0.0	109.5	3.5	130.1	5.0
2	69.9	0.3	115.0	9.7	94.1	0.5	121.4	0.0
1	56.9	0.2	66.7	3.5	74.7	4.7	72.6	3.7

Table 6 contains the most important structural parameters calculated for *tct*-2,3-DNB. At 1.363 Å, the central C1−C2 distance is, as anticipated, shorter than the one in 3,4-dimethylfuroxan (1.422 Å, see Table 1). The N−O bond lengths amount to 1.220 Å. For the C−N−O angles, values of 113.5° were obtained.

Reaction Pathway. The experimental results indicate that the first step of the photoinduced decomposition of dimethylfuroxan is the opening of the furoxan ring. This conclusion is supported by the observation that 2,3-dinitrosobut-2-ene is formed before there is any significant amount of acetonitrile-*N*-oxide. However, the exact mechanism cannot be resolved on the basis of the results provided in this study. A computational description would require extensive multireference ab initio calculations on the excited-state surface, which are beyond the scope of this study. For that very reason, the following discussion does not rely on quantitative computational results. However, the following pathway would explain our experimental observations: On the basis of the assumption that the furoxan ring will be opened by the excitation to the S_1 surface, a local minimum on the surface may correspond to an open-shell singlet. A conical intersection connecting the open-shell surface with the ground-state surface may be passed leading to closed-shell 2,3-dinitrosobut-2-ene. Because 2,3-dinitrosobut-2-ene has been trapped in our experiments after very short photolysis times, the preferred reaction path may lead directly from the open-shell singlet surface to 2,3-dinitrosobut-2-ene. In a second step, this species decomposes to acetonitrile-*N*-oxide because

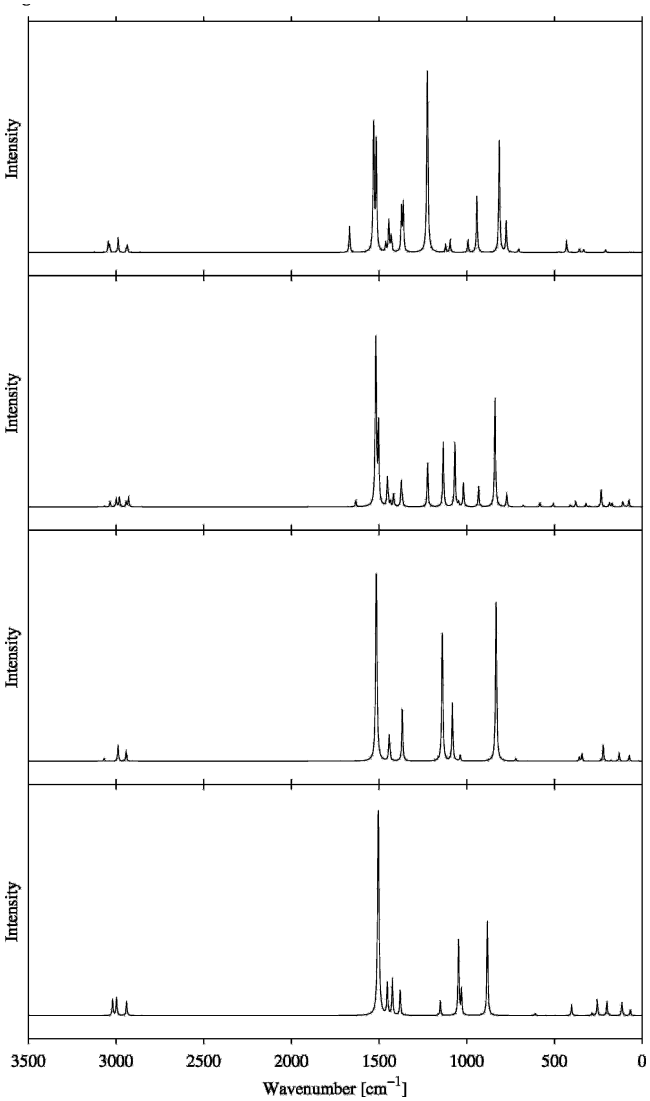

Figure 4. Simulated IR spectra of all 2,3-dinitrosobut-2-ene conformers: (top) *tct*-2,3-DNB; (2nd) *ctt*-2,3-DNB; (3rd) *ttt*-2,3-DNB; (bottom) *ctc*-2,3-DNB.

at longer photolysis times the observed IR spectrum is clearly dominated by acetonitrile-*N*-oxide.

Equation 1 shows possible pathways of the reaction. An interesting question is whether *tct*-2,3-DNB or the open-shell

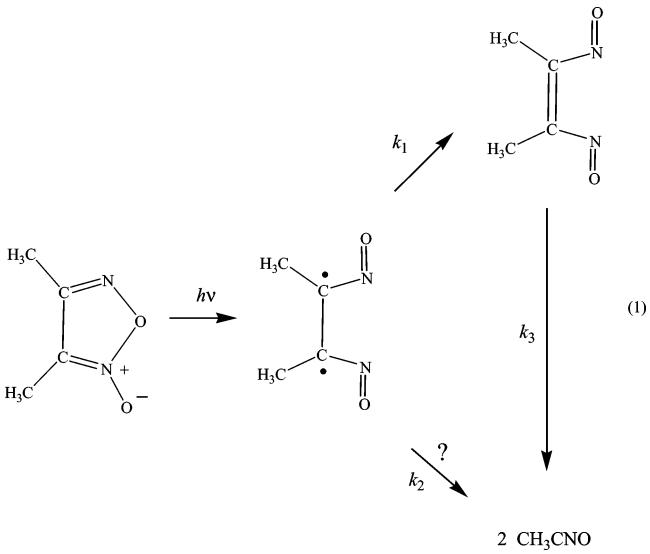

(1)

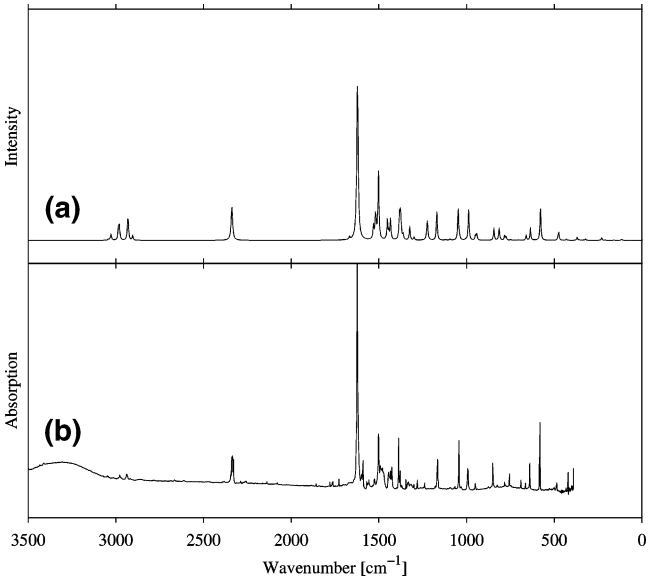

Figure 5. Comparison of (a) the experimental IR spectrum obtained following 5 min of UV photolysis of an Ar matrix containing dimethylfuroxan and (b) the superposition of the calculated IR spectra of dimethylfuroxan, *tct*-2,3-DNB, and CH_3CNO.

TABLE 6: Selected Structural Parameters of *trans-cis-trans*-2,3-Dinitrosobut-2-ene (B3LYP/cc-pVTZ)

parameter	bond length [Å]	parameter	angle [deg]
r(C1−C2)	1.363	∠(C3−C1−C2)	123.7
r(C1−C3)	1.497	∠(C4−C2−C1)	123.7
r(C2−C4)	1.497	∠(C1−C2−N2)	116.1
r(C1−N1)	1.458	∠(C2−C1−N1)	116.1
r(C2−N2)	1.458	∠(C1−N1−O1)	113.5
r(N1−O1)	1.220	∠(C2−N2−O2)	113.5
r(N2−O2)	1.220		

dinitroso species represents the direct precursor to CH_3CNO. Because *tct*-2,3-DNB is consumed upon prolonged photolysis, there must be either a direct way from this compound to CH_3CNO or a route first back to the open-shell dinitroso species, which then decomposes to give CH_3CNO. Detailed calculations are necessary to obtain more information about these two possible pathways. However, these calculations are far beyond the scope of this article.

The experiments, however, indicate that k_2 is very small. This follows from the large induction period for CH_3CNO generation. CH_3CNO can only be detected for photolysis times that also showed significant amounts of *tct*-2,3-DNB. For $k_2 = 0$, k_1 and k_3 can be derived from the experiments, if the calculated intensities are used to correlate the intensities to concentrations. It follows that $k_1 = 2.5 \times 10^{-4}$ s^{-1} and $k_3 = 2.1 \times 10^{-2}$ s^{-1}. Thus the experiments indicate that the ring-opening process is the rate-determining step of the decomposition.

According to our calculations, the reaction from dimethylfuroxan to the *tct*-dinitrosobut-2-ene (eq 2) is endothermic by 135.5 kJ mol^{-1} (146.0 kJ mol^{-1} including ZPVE corrections). It is noteworthy that the calculations predict *tct*-2,3-dinitrosobut-2-ene to be unstable toward decomposition into CH_3CNO, in agreement to what is observed in the experiments. Thus, the reaction energy for eq 3 amounts to −17.3 kJ mol^{-1} (−23.0 kJ mol^{-1} including ZPVE corrections).

In agreement with the calculations of Pasinszki and Westwood, the overall reaction from dimethylfuroxan leading to two moieties of CH_3CNO is endothermic by about 118.2 kJ mol^{-1} without and 123.0 kJ mol^{-1} with ZPVE corrections. These values are also in reasonable agreement to the experimental

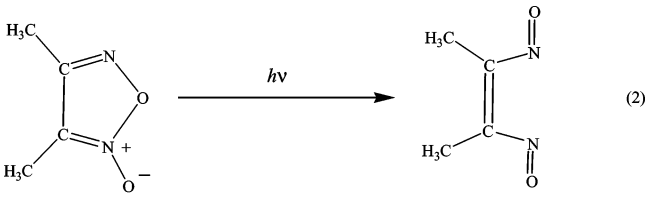

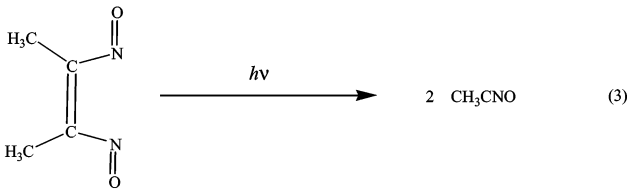

finding that dimethylfuroxan can be decomposed at elevated temperatures.

To obtain more information about the reaction pathways, an experiment was preformed in which *tct*-2,3-DNB was first generated by photolyzing the matrix for 5 min with UV light. In a second step, the matrix was photolyzed with IR light ($\lambda_{max} = 700$ nm, first 20 min, then 2 h). As a result of the second photolysis, the absorptions due to *tct*-2,3-DNB decreased, while the absorptions due to CH_3CNO increased. This might imply that the barrier to decomposition of *tct*-2,3-DNB is relatively small and is not induced by a second photoreaction. The "thermal energy" provided by the IR light is thus sufficient to cause the dinitroso species to decompose.

Conclusions

A combination of experimental and quantum chemical results was used to analyze dimethylfuroxan and its photochemistry. In the experiments, the molecules were isolated in a matrix of solid Ar at 12 K, and the matrix subsequently exposed to UV radiation. The changes induced by photolysis were monitored, and the photoproducts were characterized by IR spectroscopy. The results show that two photoproducts are formed, and these two species can be identified as 2,3-dinitrosobut-2-ene and acetonitrile-*N*-oxide. Consequently, an aliphatic open-chain dinitroso compound has been trapped for the first time which thus supports the evidence that the photochemical decomposition of dimethylfuroxan is initiated by the breakage of the endocyclic N−O bond. 2,3-Dinitrosobut-2-ene is not photostable but is transformed into the second species after prolonged photolysis times. Although it is not the most stable structure, the only conformer of 2,3-dinitrosobut-2-ene that has been identified in the Ar matrix is *trans-cis-trans*-2,3-dinitrosobut-2-ene. However, the exact mechanism of the photoreaction can only be resolved by a detailed investigation of conical intersections between the S_0 and S_1 surfaces at the multireference level.

Acknowledgment. The authors kindly acknowledge the financial support from the *Deutsche Forschungsgemeinschaft* and the award of a Habilitandenstipendium (to H.-J.H.). The authors thank the referees of this manuscript for their extremely helpful comments.

References and Notes

(1) Hwang, K.-J.; Shin, Y. A.; Jo, I.; Yoo, S.; Lee, J. H. *Tetrahedron Lett.* **1995**, *36*, 3337.
(2) Sheremetev, A. B.; Makhova, N. N.; Friedrichsen, W. *Adv. Heterocycl. Chem.* **2001**, *78*, 66.
(3) Friedrichsen, W. *J. Phys. Chem.* **1994**, *98*, 12933.
(4) Rauhut, G. *J. Comput. Chem.* **1996**, *17*, 1848.
(5) Eckert, F.; Rauhut, G.; Katritzky, A. R.; Steel, P. J. *J. Am. Chem. Soc.* **1999**, *121*, 6700.
(6) Rauhut, G.; Jarzecki, A.; Pulay, P. *J. Comput. Chem.* **1997**, *18*, 489.
(7) Friedrichsen, W. *J. Chem. Res. (S)* **1995**, 120.
(8) Friedrichsen, W. *J. Mol. Struct. (THEOCHEM)* **1995**, *342*, 23.
(9) Klenke, B.; Friedrichsen, W. *Tetrahedron* **1996**, *52*, 743.
(10) Klenke, B.; Friedrichsen, W. *J. Mol. Struct. (THEOCHEM)* **1998**, *451*, 263.
(11) Ponder, M.; Fowler, J. E.; Schaefer, H. F. *J. Org. Chem.* **1994**, *59*, 6431.
(12) Murata, S.; Tomioka, H. *Chem. Lett.* **1992**, 57.
(13) Hacker, N. P. *J. Org. Chem.* **1991**, *56*, 5216.
(14) Dunkin, I. R.; Lynch, M. A.; Boulton, A. J.; Henderson, N. *J. Chem. Soc., Chem. Commun.* **1991**, 1178.
(15) Seminario, J. M.; Concha, M. C.; Politzer, P. *J. Comput. Chem.* **1992**, *13*, 177.
(16) Stevens, J.; Schweizer, M.; Rauhut, G. *J. Am. Chem. Soc.* **2001**, *123*, 7326.
(17) Pasinszki, T.; Westwood, N. P. C. *J. Phys. Chem. A* **2001**, *105*, 1244.
(18) Mielke, Z.; Hawkins, M.; Andrews, L. *J. Phys. Chem.* **1989**, *93*, 558.
(19) Friedrichsen, W. In *Houben-Weyl. Methoden der organischen Chemie* Schaumann, E., Ed.; Thieme Verlag: Stuttgart, Germany, 1994; Hetarene III, Teil 3, Board E 8 c, p 734. There is a typographical error in this reference regarding the boiling point. It should read 107−108 °C/14 Torr.
(20) Schnöckel, H.; Schunk, S. *Chem. Unserer Zeit* **1987**, *21*, 73.
(21) Downs, A. J.; Himmel, H.-J.; Manceron, L. *Polyhedron* **2002**, *21*, 473.
(22) Himmel, H.-J.; Downs, A. J.; Greene, T. M. *Chem. Rev.* **2002**, *102*, 4191.
(23) Becke, A. D. *J. Chem. Phys.* **1993**, *98*, 1372.
(24) Lee, C.; Yang, W.; Parr, R. G. *Phys. Rev. A* **1988**, *38*, 3098.
(25) Frisch, M. J.; Trucks, G. W.; Schlegel, H. B.; Scuseria, G. E.; Robb, M. A.; Cheeseman, J. R.; Zakrzewski, V. G.; Montgomery, J. A., Jr.; Stratmann, R. E.; Burant, J. C.; Dapprich, S.; Millam, J. M.; Daniels, A. D.; Kudin, K. N.; Strain, M. C.; Farkas, O.; Tomasi, J.; Barone, V.; Cossi, M.; Cammi, R.; Mennucci, B.; Pomelli, C.; Adamo, C.; Clifford, S.; Ochterski, J.; Petersson, G. A.; Ayala, P. Y.; Cui, Q.; Morokuma, K.; Malick, D. K.; Rabuck, A. D.; Raghavachari, K.; Foresman, J. B.; Cioslowski, J.; Ortiz, J. V.; Stefanov, B. B.; Liu, G.; Liashenko, A.; Piskorz, P.; Komaromi, I.; Gomperts, R.; Martin, R. L.; Fox, D. J.; Keith, T.; Al-Laham, M. A.; Peng, C. Y.; Nanayakkara, A.; Gonzalez, C.; Challacombe, M.; Gill, P. M. W.; Johnson, B. G.; Chen, W.; Wong, M. W.; Andres, J. L.; Head-Gordon, M.; Replogle, E. S.; Pople, J. A. *Gaussian 98*, revision A.1; Gaussian, Inc.: Pittsburgh, PA, 1998.
(26) Pulay, P.; Fogarasi, G.; Pang, F.; Boggs, J. E. *J. Am. Chem. Soc.* **1979**, *101*, 2550.
(27) Rauhut, G.; Pulay, P. *J. Phys. Chem.* **1995**, *99*, 3093.
(28) Figgen, D.; Metz, B.; Stoll, H.; Rauhut, G. *J. Phys. Chem. A* **2002**, *106*, 6810.
(29) Rauhut, G.; Werner, H.-J. *Phys. Chem. Chem. Phys.* **2003**, *5*, 2001.
(30) Dunkin, I. R.; Lynch, M. A.; Boulton, A. J.; Henderson, N. *J. Chem. Soc., Chem. Commun.* **1991**, 1178.